# Nanodomain structures formation during polarization reversal in uniform electric field in strontium barium niobate single crystals

V. Ya. Shur, V. A. Shikhova, A. V. Ievlev, P. S. Zelenovskiy, M. M. Neradovskiy, D. V. Pelegov, and L. I. Ivleva

Citation: Journal of Applied Physics **112**, 064117 (2012); doi: 10.1063/1.4754511
View online: http://dx.doi.org/10.1063/1.4754511
View Table of Contents: http://scitation.aip.org/content/aip/journal/jap/112/6?ver=pdfcov
Published by the AIP Publishing



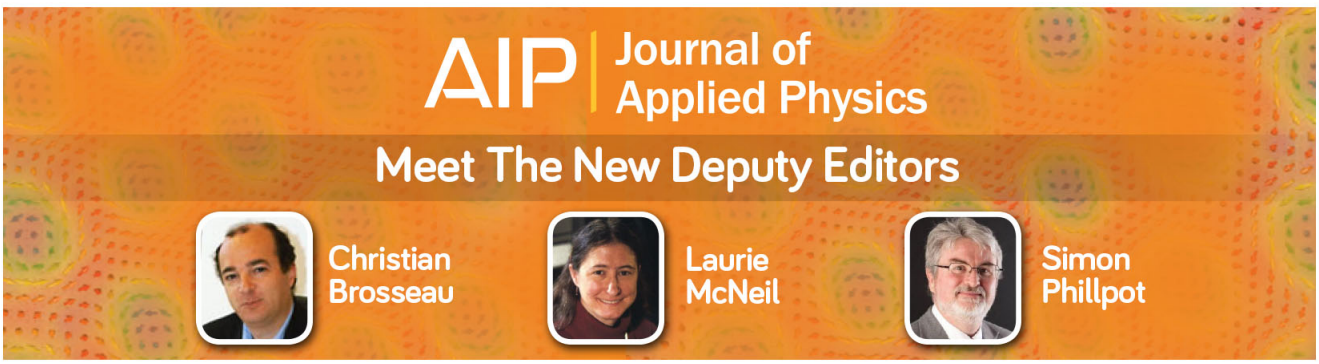

# Nanodomain structures formation during polarization reversal in uniform electric field in strontium barium niobate single crystals

V. Ya. Shur,[1,a)] V. A. Shikhova,[1] A. V. Ievlev,[1] P. S. Zelenovskiy,[1] M. M. Neradovskiy,[1] D. V. Pelegov,[1] and L. I. Ivleva[2]
[1]*Ferroelectric Laboratory, Institute of Natural Sciences, Ural Federal University, 620000 Ekaterinburg, Russia*
[2]*Prokhorov General Physics Institute, Russian Academy of Sciences, 119991 Moscow, Russia*

(Received 2 July 2012; accepted 24 August 2012; published online 26 September 2012)

We have studied the ferroelectric nanodomain formation in single crystals of strontium barium niobate $Sr_{0.61}Ba_{0.39}Nb_2O_6$ using piezoelectric force microscopy and Raman confocal microscopy. The nanodomain structures have been created by application of the uniform electric field at room temperature. Four variants of nanodomain structure formation have been revealed: (1) discrete switching, (2) incomplete domain merging, (3) spontaneous backswitching, and (4) enlarging of nanodomain ensembles. Kinetics of the observed micro- and nanodomain structures has been explained on the basis of approach developed for lithium niobate and lithium tantalate crystals. © *2012 American Institute of Physics*. [http://dx.doi.org/10.1063/1.4754511]

## I. INTRODUCTION

In recent years, the domain structure of uniaxial ferroelectrics have been carefully studied due to possibility of their application in optoelectronics, nonlinear optics, piezoelectricity, and, especially, for frequency conversion devices based on periodic domain structures. The study of the kinetics of nanoscale domains in lithium niobate (LN) and lithium tantalate (LT) single crystals has been stimulated by their important applications for creation of new nonlinear optical devices.[1] At the same time, the uniaxial relaxor ferroelectric strontium barium niobate ($Sr_xBa_{1-x}Nb_2O_6$, SBN) considered as a prospective material for domain engineering is still not studied enough. The prominent electro-optical properties of SBN together with high values of dielectric permittivity and piezoelectric coefficients[2] open new horizons for commercialization of the domain patterned crystals. On the other hand, it is considered that the nanoscale inhomogeneity of chemical composition in relaxor ferroelectrics complicated the domain engineering SBN.[3]

First high resolution study of the static domain structure in SBN was carried out in 1986 and represents visualization of wedge-like 180° domains at [100] SBN crystal surface at room temperature by dark-field electron microscopy.[4] Further high-resolution studies of the static domain patterns on the polar surface of pure and doped SBN crystals were performed by scanning probe microscopy.[5–7] In particular, piezoresponse force microscopy (PFM) allowed revealing the maze-type ("island") initial domain structures with characteristic sizes about hundred nanometers[6] in thermally depolarized SBN single crystals, as well as the evolution of the initial domain structure at different temperatures.[7] Recently, the micro- and nanodomain structures formed in SBN during polarization reversal in uniform field were studied using PFM.[8] Moreover, the stability of microdomains and microdomain arrays recorded in SBN under the action of highly nonuniform field produced by the tip of scanning probe microscope was studied.[9]

There are only a few publications devoted to investigation of the domain kinetics in SBN. At the beginning the domain kinetics in SBN was studied using decoration by nematic liquid crystals.[10] Recently, electro-optic imaging microscopy has been used for investigation of micron-scale domain nucleation and growth in SBN61 single crystals by dc electric-field pulses.[11–13]

The high-resolution methods can be applied for studying the static domain structures only, while optical methods cannot provide *in situ* domain visualization with nanoscale resolution. Recently, the Raman confocal microscopy (RCM) has been used for obtaining the domain images in the crystal bulk and for reconstructing the domain kinetics in LN and LT crystals.[14,15]

In this work, the formation of the nanodomain structures in $Sr_{0.61}Ba_{0.39}Nb_2O_6$ slightly doped by Ce during switching in uniform electric field applied by liquid electrodes has been revealed by the domain image obtained by PFM and RCM methods. The formation of the obtained domain structures has been explained in framework of the approach developed for uniaxial LN and LT crystals.

## II. EXPERIMENTAL

The studied samples represented plates of strontium barium niobate $Sr_{0.61}Ba_{0.39}Nb_2O_6$ doped by 0.004 wt. % $CeO_2$ (SBN61:Ce) single crystal grown by modified Stepanov technique[16] in Institute of General Physics of the Russian Academy of Sciences. The 0.5-mm-thick plates were cut normally to the polar axis and carefully polished. All measurements were carried out at room temperature, which was essentially lower than the freezing temperature for the studied composition ($T_f = 60\,^{\circ}C$).[17]

Two variants of single domain state preparation were used: (1) thermal polarization in constant field and (2)

a)Author to whom correspondence should be addressed. Electronic mail: vladimir.shur@usu.ru.

 

application of bipolar pulses. The uniformity of the created domain state was verified by PFM.

The thermal polarization was carried out in constant field ($E = 700$ V/mm) applied using e-beam evaporated Cr electrodes during cooling from 180 °C to room temperature with cooling rate 5 °C/min. The Cr electrodes were removed by chemical etching before switching using liquid electrodes.

The application of 30–50 bipolar rectangular or triangular field pulses with amplitude and duration sufficient for complete polarization reversal at room temperature using liquid electrodes also allowed obtaining the single domain state.

The subsequent polarization reversal in uniform electric field was performed by bipolar rectangular electric field pulses using the cell with liquid electrodes described in Ref. 12. The field pulses were generated by DAC board PCI-6251 (National Instruments, USA) controlled by the original software and amplified by a high voltage amplifier Trek 677B (TREK, USA).

The domains at the surface were visualized by PFM using Probe NanoLaboratory NTEGRA Aura (NT-MDT, Russia) with the silicon DCP20 and DCP11 tips (NT-MDT, Russia) having diamond-like conductive coating and typical radius of curvature about 50 nm. AC modulation voltage with amplitude $U_{mod} = 1 \div 3$ V and frequency $f_{mod} = 12.5 \div 17.4$ kHz was applied between the conductive tip and bottom electrode to invoke the piezoelectric response of the surface.[18]

The domain walls in the bulk were visualized by RCM using Probe NanoLaboratory NTEGRA Spectra (NT-MDT, Russia), which consisted of high resolution confocal scanning laser microscope, Raman spectrometer, and atomic-force microscope. The He-Ne laser with $\lambda = 633$ nm and power 50 mW was used as a pumping source.[15] Laser focusing was performed by objective $\times 100$ with numerical aperture 0.95 mounted in inversed optical microscope Olympus IX71. A diffraction grating 600 dash/mm with spectral resolution 2.27 $cm^{-1}$ at $\lambda = 633$ nm was used for light decomposition. The estimated achieved lateral resolution of RCM was below 300 nm and resolution in depth was about 500 nm.[15]

It has been shown by us that in SBN the frequency of $A_{1g}$ Raman band located around 592 $cm^{-1}$ changes up to 6 $cm^{-1}$ in the vicinity of the domain walls. The similar effect revealed in LN and LT crystals has been used successively for visualization of the domain walls in the bulk.[14,15] In order to obtain the domain wall images, the Raman spectra were recorded in adjacent points with the step 100 nm within a 2D scanning at the crystal surface and in the bulk at the different depths (distance from the polar surface). The frequency of $A_{1g}$ band in each point was identified by fitting of the Raman spectrum and its spatial distribution was converted into 2D digital arrays and represented in gray-scale or pseudo-color images.

## III. RESULTS AND DISCUSSION

It has been shown that the shape of domains formed during switching in uniform field in SBN crystals essentially depends on the switching conditions. Let us consider separately the typical micro- and nanodomain structures obtained for switching in low and high fields and for spontaneous backswitching after external field switch off.

### A. Low electric field

#### 1. Square domains

The typical PFM image of the domain structure for switching by single low field pulse (amplitude 340 V/mm, duration 1 s) obtained in the central part of the switched area consists of isolated and merged regular-shaped square-like domains (Fig. 1). The square shape correlates with $C_{4v}$ crystals symmetry[1,2,19] and has been observed at first in $BaTiO_3$ crystals.[20]

The regular domain shape can be explained using the model of isolated domain growth in crystals of LN and LT family.[1,19] In LN with $C_{3V}$ symmetry, the domains demonstrate hexagon shape with walls strictly oriented along Y crystallographic directions. Such behavior has been attributed to the determined nucleation mechanism, which means the inhomogeneous step generation along the wall.[19] The switching field at the moving wall is decreased due to incomplete screening of depolarization field. This screening retardation leads to formation of the field singularities at the polygon vertices for polygon domain shape, causing local increase of the step generation probability. The direct experimental observation of the domain kinetics in LN allows to state that the steps were generated at the polygon vertices and propagated along Y direction.[21] Thus, the hexagon domain shape is observed experimentally during slow switching in LN. In crystals of $C_{4v}$ symmetry, the mechanism of determined nucleation has to result in growth of the square domains.

#### 2. Formation of the residual domains during merging

It has been shown that the residual domains persist after domain merging along the lines of the domain contact in SBN (Fig. 1). It is necessary to point out that the similar formation of the residual domains during merging has been

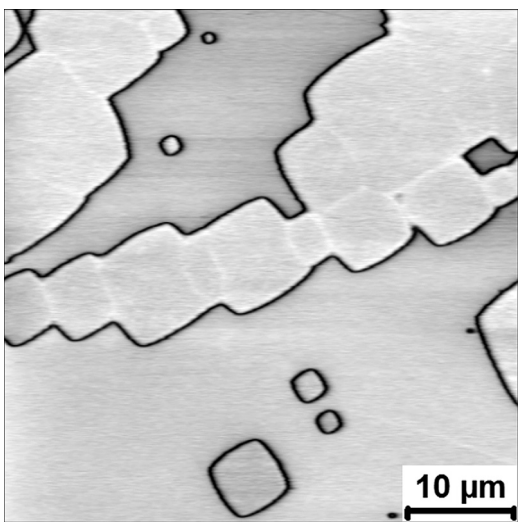


FIG. 1. Typical domain structure produced in SBN by switching in low field ($E = 340$ V/mm) in the central part of the switched area. PFM image. Amplitude of piezoresponse signal.

revealed in congruent LN (CLN) with surface layer modified by proton exchange and has been never obtained during domain kinetics in CLN during "equilibrium" switching.[22]

This effect can be explained while taking into account the "electrostatic interaction" between approached domain walls for incomplete screening of the depolarization field. In this case, the trail of residual depolarization field ($E_{rd}$) existing above the moving domain wall decelerates the counter motion of the domain walls before merging and stimulates the formation of the chains of isolated domains. The formation of the residual domains has been observed earlier in CLN crystals with the artificial dielectric gap produced by proton exchange, which leads to increase of the residual depolarization field due to ineffective external screening.[1,19,22] This was the reason for us to study the domain kinetics in SBN for switching with ineffective external screening due to low conductive (poor quality) electrode.

### 3. Ineffective external screening

The switching with ineffective external screening has been realized in the vicinity of the boundary of liquid electrode representing the area with very thin and low conductive electrolyte layer. It is clearly seen that the domain kinetics in these areas (Figs. 2 and 3) drastically differs from the one observed in the central part of the switched area (Fig. 1). The observed discrete switching represents (1) formation of the nanodomain chains in front of the moving domain wall (Fig. 2) and (2) enlargement of the nanodomain ensembles (Fig. 3). The similar discrete switching effect has been observed in lithium niobate crystals for highly non-equilibrium switching conditions caused by ineffective external screening.[19]

The formation of the isolated needle-like nanodomains and their growth in front of the moving domain wall have been observed in SBN in low field ($E = 340$ V/mm) (Fig. 2). In this case, the domain wall became very rough due to merging with formed isolated nanodomains. The nanodomains of typical diameter $40 \div 80$ nm have appeared at the averaged distance from the domain wall not exceeding 200 nm. The obtained effect can be attributed to correlated nucleation caused by ineffective screening of the depolarization field.[1,19]

It has been shown by numerical simulations that the spatial distribution of the residual depolarization field $E_{rd}$ in the vicinity of the domain wall demonstrates a pronounced maximum at the distance from the wall about the thickness of the dielectric gap.[21] The $E_{rd}$ maximum increases essentially the 3D-nucleation probability in front of the wall, thus leading to nucleation of isolated nanodomains. Subsequent growth of the nanodomains and their merging with domain wall lead to formation of irregular domain wall shape (lack of the domain shape stability) (Fig. 2).

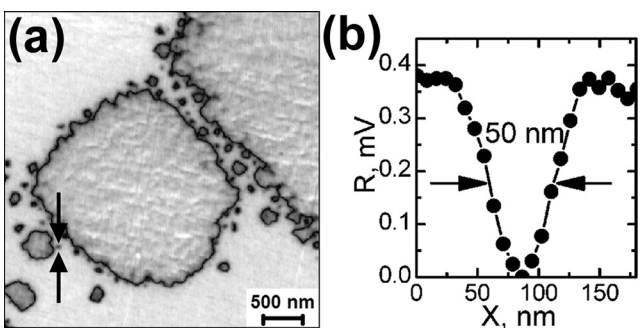


FIG. 2. (a) Discrete switching in front of the moving domain wall in SBN in the vicinity of the edge of liquid electrode. Switching in low field ($E = 340$ V/mm). PFM image. Amplitude of piezoresponse signal. (b) Domain profile marked in panel (a).

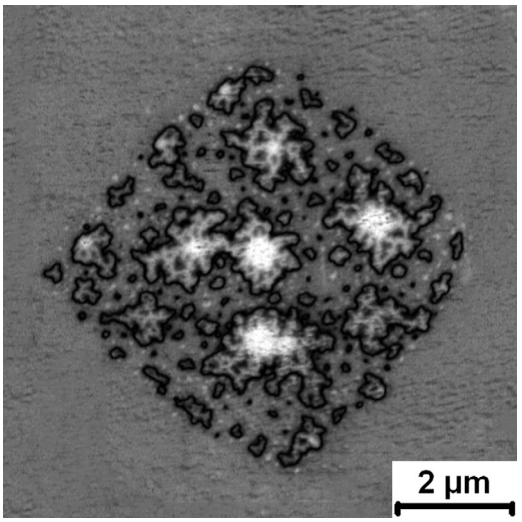


FIG. 3. Typical domain ensemble produced in SBN in the vicinity of the edge of liquid electrode by switching in low field ($E = 340$ V/mm). PFM image. Amplitude of piezoresponse signal.

Moreover, the "nanodomain ensembles" representing quasi-regular structures consisting of isolated nanodomains and irregular-shaped micro-domains have been also formed and enlarged in the vicinity of the electrode boundary (Fig. 3). The square shape of the whole domain ensembles was similar to the shape of isolated domains in the center of the switched area. The minimal diameter of isolated nanodomains in ensemble was about 60 nm (Fig. 3). In this case, the kinetics of domain structure is not a classical growth of homogeneous domains due to the sideways motion of the domain walls. Increasing of the ensemble area is due to the discrete switching—appearance of isolated nanodomains in the vicinity of the ensemble boundary.

The formation and growth of similar nanodomain ensembles with diameter of nanodomains about 50 nm and distance between the nanodomain walls about 100 nm have been observed also in SBN crystals after thermal polarization in constant field in the central part of the switched area (Fig. 4).

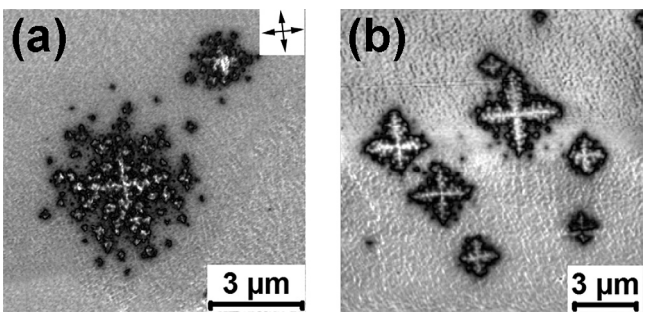


FIG. 4. Typical domain ensemble produced in SBN after thermal polarization by switching in low field ($E = 340$ V/mm) in the central part of the switched area. PFM image. Amplitude of piezoresponse signal.

The formation and growth of the nanodomain ensembles with the shape close to the shape of isolated micron-scale domains have been observed previously for completely ineffective screening conditions in CLN and stoichiometric LT with artificial surface dielectric layer obtained by proton exchange and by photoresist layer deposited on the crystal surface.[1,19] It has been shown that the average distance between the nearest isolated domains in the ensemble is equal to the thickness of artificial dielectric layer, which is caused by the correlated nucleation effect.[1,19] The period of the domains appeared in CLN during discrete switching without artificial dielectric gap (about 100 nm) was attributed to the thickness of the intrinsic effective gap.[1] This fact allows us to assume that in SBN, the thickness of the intrinsic effective dielectric gap is about 100–200 nm.

### B. High electric field

Increase of the applied field pulse amplitude resulted not only in usual acceleration of the switching process but also in formation of circular domains with wide nanodomain band in front of the moving wall (Fig. 5). The irregular and circle domain shapes indicates the dominance of the stochastic nucleation.[19] The observed effects can be attributed to ineffective screening of depolarization field during fast switching. The ineffective screening leads to deceleration and suppression of the sideways domain wall motion when the formation of isolated nanodomains in front of the moving domain wall prevails.[19] In this case, the step generation is caused by merging of the isolated nanodomains with the domain wall. Such equiprobable step generation (stochastic nucleation) results in irregular wall shape and isotropic domain growth.

### C. Spontaneous backswitching

The nanodomain formation has been obtained also as a result of the spontaneous backswitching (flip-back) after fast external field switch off. The formation of shallow nanodomain structures in the surface layer of the freshly switched micro-domains as a result of the backswitching effect has been revealed by PFM (Fig. 6(a)). The effect has been caused by action of the residual depolarization field inside the fresh domain.[23]

Additional information about the nanodomain structures in the bulk has been obtained by RCM (Figs. 6(b)–6(d)). The high contrast caused by frequency shift of RCM signal obtained at the surface over almost whole domain area (except domain center) (Fig. 6(b)) has testified the high concentration of the charged domain walls. The obtained contrast has decreased with the depth (Fig. 6(c)) and has disappeared at about 25 $\mu$m (Fig. 6(d)). This fact allows to state that the depth of the backswitched domains is below 25 $\mu$m. Moreover, the set of the domain images at the different depths can be used for extracting the scenario of the domain structure formation.[15] It has been revealed that the backswitching process starts from formation of the nanodomains along the wall of existing domain and continues to its center (Figs. 6(b)–6(d)).

It is necessary to point out that all observed mechanisms of nanodomain structure formation: (a) incomplete domain merging (Fig. 7(a)), (b) discrete switching (Fig. 7(b)), (c) spontaneous backswitching (Fig. 7(c)), and (d) enlarging of nanodomain ensembles (Fig. 7(d)), have been observed earlier in crystals of LN and LT family.[1,19,21–23] This fact allows us to state that the evolution of the domain structure in single crystals of uniaxial relaxor ferroelectric SBN during switching in ferroelectric phase is similar to normal uniaxial ferroelectrics LN and LT in spite of inhomogeneity of the chemical composition in SBN.

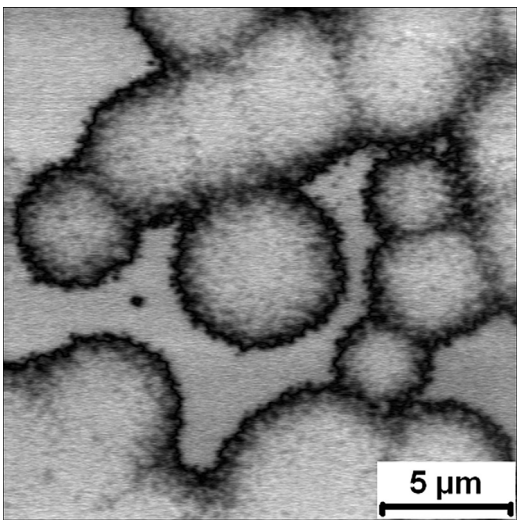


FIG. 5. Discrete switching in front of the moving domain wall in SBN in high field ($E = 680$ V/mm) in the central part of the switched area. PFM image. Amplitude of piezoresponse signal.

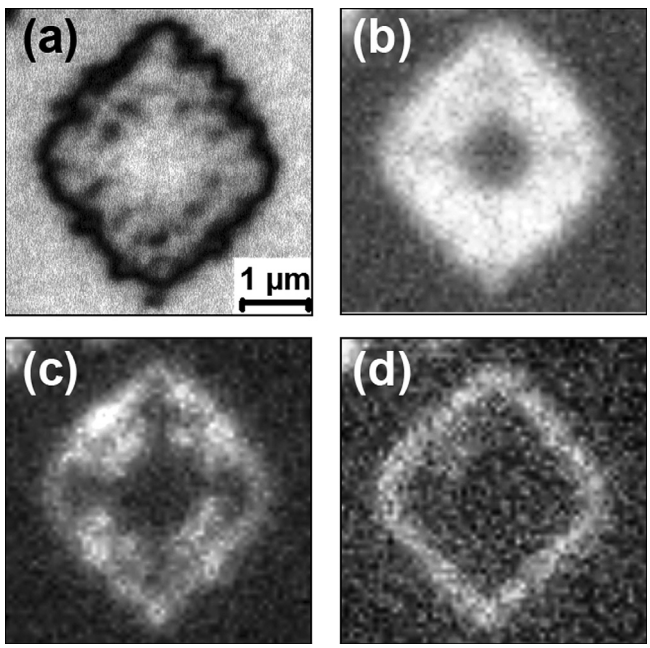


FIG. 6. Images of nanodomain ensemble appeared as a result of spontaneous backswitching in SBN ((a) and (b)) at the surface and ((c) and (d)) in the bulk. Visualization by (a) PFM at the surface. ((b)–(d)) RCM at different depths: (b) at the surface, (c) 10 $\mu$m, (d) 25 $\mu$m.

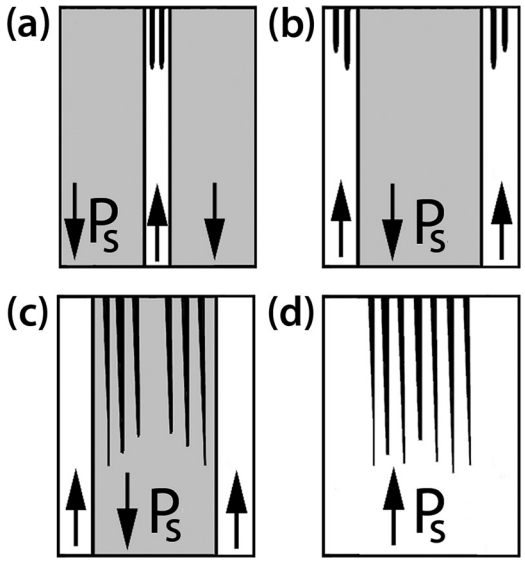


FIG. 7. The scheme of the domain structures formed by (a) incomplete merging, (b) discrete switching, (c) spontaneous backswitching, (d) enlarging of nanodomain ensembles.

## IV. CONCLUSIONS

The formation of nanodomain structures during polarization reversal in uniform electric field in single crystals of relaxor ferroelectric strontium barium niobate ($Sr_{0.61}Ba_{0.39}Nb_2O_6$), slightly doped by Ce was investigated. The single-domain state was created in the surface layer by application of series of ac electric field pulses or by thermal polarization during cooling in dc field. It was shown that the nanodomain structure formation occurred as a result of (1) discrete switching, (2) incomplete merging, (3) spontaneous backswitching, and (4) growth of nanodomain ensembles. The increasing of applied field resulted in the formation of circular domains with wide nanodomain band in front of the moving wall, thus leading to isotropic domain growth. The observed effects were attributed to ineffective screening of depolarization field. Kinetics of the observed domain structure was explained by approach developed for LN and LT crystals. It was shown that the domain structure evolution in SBN during switching in ferroelectric phase was the same as in LN and LT.

## ACKNOWLEDGMENTS

The equipment of the Ural Center for Shared Use "Modern Nanotechnology," Institute of Natural Sciences, Ural Federal University has been used. The research was made possible in part by RFBR (Grants 10-02-96042-r-Ural-a, 10-02-00627-a, 11-02-91066-CNRS-a), by Ministry of Education and Science (Contracts 16.740.11.0585 and 16.552.11.7020), by the Program "Scientific and scientific pedagogical personnel of innovative Russia 2009–2013," by OPTEC LLC and in terms of the Ural Federal University development program with the financial support of young scientists.

[1]V. Ya. Shur, J. Mater. Sci. **41**, 199 (2006).
[2]A. M. Prokhorov and Yu. S. Kuz'minov, *Ferroelectric Crystals for Laser Radiation Control* (Adam Hilger, Bristol, 1990).
[3]G. A. Samara, J. Phys.: Condens. Matter **15**, R367 (2003).
[4]L. A. Bursill and P. J. Lin, Philos. Mag. B **54**, 157 (1986).
[5]P. Lehnen, W. Kleemann, Th. Woike, and R. Pankrath, Phys. Rev. B: Condens. Matter **64**, 224109 (2001).
[6]K. Terabe, S. Takekawa, M. Nakamura, K. Kitamura, S. Higuchi, Y. Gotoh, and A. Gruverman, Appl. Phys. Lett. **81**, 2044 (2002).
[7]J. Dec, V. V. Shvartsman, and W. Kleemann, Appl. Phys. Lett. **89**, 212901 (2006).
[8]V. Ya. Shur, V. A. Shikhova, D. V. Pelegov, A. V. Ievlev, and L. I. Ivleva, Phys. Solid State **53**, 2311 (2011).
[9]T. R. Volk, L. V. Simagina, R. V. Gainutdinov, A. L. Tolstikhina, and L. I. Ivleva, J. Appl. Phys. **108**, 042010 (2010).
[10]N. R. Ivanov, T. R. Volk, L. I. Ivleva, S. P. Chumakova, and A. V. Ginzberg, Crystallogr. Rep. **47**, 1023 (2002).
[11]L. Tian, D. A. Scrymgeour, and V. Gopalan, J. Appl. Phys. **97**, 114111 (2005).
[12]V. Ya. Shur, D. V. Pelegov, V. A. Shikhova, D. K. Kuznetsov, E. V. Nikolaeva, E. L. Rumyantsev, O. V. Yakutova, and T. Granzow, Ferroelectrics **374**, 33 (2008).
[13]V. Ya. Shur, D. V. Pelegov, V. A. Shikhova, D. K. Kuznetsov, E. V. Nikolaeva, E. L. Rumyantsev, O. V. Yakutova, and T. Granzow, Phys. Solid State **52**, 346 (2010).
[14]P. Zelenovskiy, M. Fontana, V. Shur, P. Bourson, and D. Kuznetsov, Appl. Phys. A **99**, 741 (2010).
[15]V. Ya. Shur, P. S. Zelenovskiy, M. S. Nebogatikov, D. O. Alikin, M. F. Sarmanova, A. V. Ievlev, E. A. Mingaliev, and D. K. Kuznetsov, J. Appl. Phys. **110**, 052013 (2011).
[16]L. I. Ivleva, Bull. Russ. Acad. Sci. Phys. **73**, 1338 (2009).
[17]T. R. Volk, V. Yu. Salobutin, L. I. Ivleva, N. M. Polozkov, R. Pankrath, and M. Woehlecke, Phys. Solid State **42**, 2129 (2000).
[18]V. Ya. Shur, A. V. Ievlev, E. V. Nikolaeva, E. I. Shishkin, and M. M. Neradovskiy, J. Appl. Phys. **110**, 052017 (2011).
[19]V. Ya. Shur, in *Handbook of Advanced Dielectric, Piezoelectric and Ferroelectric Materials: Synthesis, Properties and Applications*, edited by Z.-G. Ye (Woodhead, Cambridge, England, 2008), pp. 622–669.
[20]R. C. Miller and A. Savage, Phys. Rev. **115**, 1176 (1959).
[21]V. Ya. Shur, in *Nucleation Theory and Applications*, edited by J. W. P. Schmelzer (Wiley-VCH, Weinheim, 2005), pp. 178–214.
[22]V. Ya. Shur, E. L. Rumyantsev, A. G. Shur, A. I. Lobov, D. K. Kuznetsov, E. I. Shishkin, E. V. Nikolaeva, M. A. Dolbilov, P. S. Zelenovskiy, K. Gallo, and M. P. De Micheli, Ferroelectrics **354**, 145 (2007).
[23]V. Ya. Shur, E. L. Rumyantsev, E. V. Nikolaeva, E. I. Shishkin, D. V. Fursov, R. G. Batchko, L. A. Eyres, M. M. Fejer, and R. L. Byer, Appl. Phys. Lett. **76**, 143 (2000).